Nanoscale

PAPER

Cite this: *Nanoscale*, 2017, **9**, 2633

Highly transparent AgNW/PDMS stretchable electrodes for elastomeric electrochromic devices†

Huan-Shen Liu, Bo-Cheng Pan and Guey-Sheng Liou*

Received 27th November 2016,
Accepted 13th January 2017

DOI: 10.1039/c6nr09220a

rsc.li/nanoscale

Stretchable conductors based on silver nanowires (AgNWs) and polydimethylsiloxane (PDMS) have been studied extensively for many years. However, it is still difficult to achieve high transparency with low resistance due to the low attractive force between AgNWs and PDMS. In this paper, we report an effective method to transfer AgNWs into PDMS by using substrates which have a hydrophobic surface, and successfully prepared stretchable AgNW/PDMS electrodes having high transparency and low sheet resistance at the same time. The obtained electrodes can be stretched, twisted, and folded without significant loss of conductivity. Furthermore, a novel elastomeric HV electrochromic device (ECD) fabricated based on these stretchable AgNW/PDMS hybrid electrodes exhibited excellent electrochromic behavior in the full AgNW electrode system and could change color between colorless and blue even after 100 switching cycles. As most existing electrochromic devices are based on ITO and other rigid conductors, elastomeric conductors demonstrate advantages for next-generation electronics such as stretchable, wearable, and flexible optoelectronic applications.

Introduction

Over the past decade, the development of a transparent conductor (TC) has seen significant progress. Among these TC materials, the most commonly used material in the current market is indium tin oxide (ITO) which could be applied widely in both research and industry for optoelectronic applications, such as transparent displays, smart windows, photovoltaic panels, and other applications. Although ITO has considerable advantages both in terms of electrical and optical properties, its drawbacks of high cost and brittleness are crucial problems that need to be improved.[1] Therefore, some novel alternative materials have attracted great attention such as carbon nanotubes (CNTs),[2] graphene,[3] and metallic nanowires.[4] Within these candidates, silver nanowires (AgNWs) clearly have progressed to be the head of the pack, with performance and cost advantages over ITO.[5] Recently, AgNW-based TCs have been intensively studied not only for applications in highly transparent conductors, but also in combination with some flexible substrates. Many groups have already investigated different kinds of AgNW/polymer electrodes, such as polyester-types,[6] poly(methyl methacrylate)-types,[7,8] polycarbonate-types,[9,10] and a variety of other polymers,[11–15] and greatly enhance the overall performance. Recently, we also reported AgNW–polyimide flexible electrodes with high transparency and thermal stability.[16,17] However, the advantages of AgNWs should not be limited to high transparency and thermal stability; the unique nature could be further emphasized for pursuing opportunities as stretchable and wearable applications.

Stretchable conductors have received considerable attention for use in the metallic parts of stretchable electronic devices. In order to achieve both conductivity and stretchability, conductive solid fillers were typically embedded in a stretchable polymer matrix in the form of bulk composites. Common stretchable polymer matrices include polyurethane (PU),[18,19] poly(styrene-*block*-butadiene-*block*-styrene) (SBS),[20] polystyrene–polyisoprene–polystyrene (SIS),[21] and poly(dimethylsiloxane) (PDMS).[22,23] Stretchable conductors based on the polymers mentioned above and conductive fillers (such as AgNWs) have been published by many groups and even have reached the commercial stage. However, it is difficult to achieve high transparency and conductivity at the same time in these typically stretchable electrodes, which may be the thin AgNW network could not be effectively transferred and embedded into the stretchable matrix resulting in lower conductivity. For this reason, rarely would a stretchable conductor be emphasized for its transparency based on high conductivity. Recently, a stretchable and transparent conductor was

Institute of Polymer Science and Engineering, National Taiwan University, Taipei, Taiwan 10617. E-mail: gsliou@ntu.edu.tw

†Electronic supplementary information (ESI) available: Experimental section; table: solubility behavior, and thermal properties of PDMS; figure: TGA, AFM and SEM photos of PDMS, high aspect ratio AgNWs, and AgNW/PDMS hybrid films. See DOI: 10.1039/c6nr09220a

first demonstrated by Pei and co-workers[13,24] using AgNWs and poly(acrylate) to achieve transparency (92%) and conductivity (50 Ω sq^{-1}) at the same time. However, the hybrid conductor has to be heated above the glass transition temperature of the polymer (above room temperature) to achieve stretchability. Moreover, Lee's group used Zonyl fluorosurfactant to improve the bonding between the functional NWs and the PDMS matrix, thus enabling highly efficient transfer of NW structures into PDMS.[25] Until now, there have been only very limited reports related to stretchable conductors with high transparency.[26,27]

Herein, highly transparent and stretchable electrodes were prepared by using the hybrid technique of high FoM value AgNWs and elastomer PDMS. By using a facile and direct method to effectively transfer the AgNWs into the PDMS substrate, we successfully fabricated electrochromic devices (ECD) by using these electrodes. This innovative approach for the first elastomeric ECD prepared by using a full AgNW system is just a representative example to manifest its applicability for stretchable or wearable optoelectronics.

Experimental

Materials

PDMS was prepared by mixing the base and curing agent (SYLGARD® 184, Dow Corning) with a ratio of 10 : 1, and the liquid mixture was degassed. Heptyl viologen tetrafluoroborate $HV(BF_4)_2$ was prepared as follows: 1.00 g $HVBr_2$ was dissolved in 10 mL DI water and dropped in 10 mL saturated $NaBF_4$ aqueous solution. After mixing, a white solid of $HV(BF_4)_2$ could be obtained after filtration, and then purified by recrystallization from ethanol.[28] Tetrabutylammonium perchlorate (TBAP) (Acros) was recrystallized twice by using ethyl acetate under a nitrogen atmosphere and then dried in a vacuum oven prior to use. Silver nitrate (99.85%, Acros), polyvinylpyrrolidone (PVP) (MW = 1 300 000, Alfa Aesar), ethylene glycol (EG) (SHOWA), copper(II) chloride (98%, SHOWA), iron(III) chloride (97%, SHOWA), and all other reagents and solvents were used as received from commercial sources.

Silver nanowire synthesis

The AgNWs were prepared by the modified polyol process which adopts PVP as a capping agent and EG as a reductant to reduce the silver nitrate.[17,29] The obtained AgNWs and SEM morphology are shown in Fig. S1.†

AgNW/PDMS stretchable electrode fabrication

The schematic diagram of the fabrication procedure for the AgNW/PDMS hybrid electrode is depicted in Fig. 1. Various concentrations of the AgNW/ethanol solution were firstly spray-coated by using an airbrush gun (nozzle diameter: 0.35 mm) on the 5.0 × 5.0 cm^2 Teflon plate which was preheated at 120 °C on a hotplate. The back pressure was set at 15 psi with a spraying distance of 15 cm from the surface of the Teflon plate. The AgNW network was annealed at 200 °C

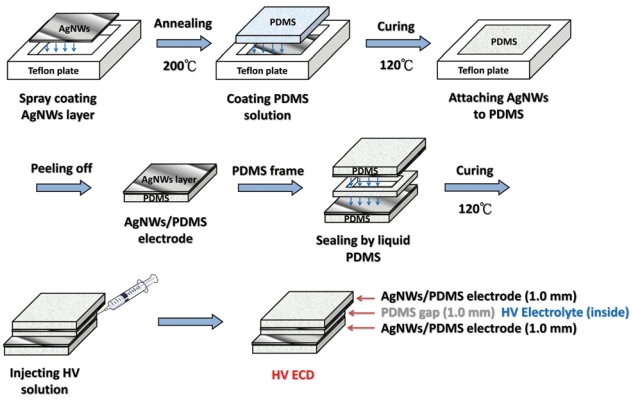

Fig. 1 Schematic diagram of the fabrication of AgNW/PDMS hybrid electrodes and elastomeric HV ECDs.

for 20 min to remove the polyvinylpyrrolidone (PVP) capping agent on the AgNW surface and produce fusion between the AgNWs. After that, the above PDMS viscous liquid was poured onto a Teflon plate. The Teflon plate was subsequently placed in an oven and cured for about 1 h at 120 °C. After curing in the oven, the AgNW/PDMS hybrid film was lifted off from the Teflon plate and a stretchable conductive layer on the other side was obtained. The total thickness of the resulting hybrid films was controlled to be around 1.0 mm.

Elastomeric electrochromic device fabrication

The preparation of electrochromic devices based on the AgNW/PDMS hybrid electrodes is listed as follows: the prepared AgNW/PDMS electrodes were placed in the lowest layer. After loading PDMS liquid within a syringe, the syringe was used to dispense the PDMS liquid on the AgNW/PDMS electrodes as an adhesive to form a frame. Next, another cured PDMS frame was placed on the AgNW/PDMS electrode as a gap, and then the PDMS liquid was dispensed on the other side of the PDMS frame. The other AgNW/PDMS electrode was placed on the top, and then placed in the oven to cure the adhesive PDMS for 1 h at 120 °C. Finally, a syringe was used to inject the solution of HV with an electrolyte (0.005 M in CH_3CN with 0.1 M of TBAP as a supporting electrolyte) into the device.

Results and discussion

Basic characterization

The characterization of instruments and measurement conditions are shown in the ESI.† PDMS is one of the most promising materials for stretchable electronics with good biocompatibility, high stretchability at room temperature, excellent optical transparency, and excellent moldability.[30,31] Moreover, its thermal stability and chemical resistance are also outstanding.[32] As shown in Fig. S2 and Table S1,† the T_d^5 and T_d^{10} of PDMS were up to 410 °C under both nitrogen and air conditions owing to the high number of Si–O bonds in the structure (the Si–O bond (460 kJ mol^{-1}) is relatively stable when

compared to the C–C bond (332 kJ mol^{-1})). And the solubility of PDMS is summarized in Table S2.† The cured PDMS film exhibited poor solubility in common organic solvents such as DMAc and NMP. Thus, using the organic-insoluble PDMS as the AgNW binder, the obtained AgNW/PDMS electrodes could enhance the potential to endure additional post-processing. Furthermore, one of the most important advantages of PDMS is its excellent optical transparency. Compared with glass and high transparency PI, PDMS has higher transparency, particularly in the range of 300–400 nm (as shown in Fig. S3†). The feature of highly colorless and optical transparency makes it more competitive in TC applications.

Properties of flexible and transparent AgNW/PDMS hybrid electrodes

The microstructures of the obtained AgNW/PDMS electrodes are depicted in Fig. 2 and S4.† AgNWs with a uniform network structure on the surface of the PDMS substrate by spraying and transferring techniques could be observed from the SEM images. As shown in Fig. 3, upon spraying AgNWs onto the hydrophobic Teflon plate, AgNWs had a weak attractive force with the Teflon plate and could easily be transferred from the Teflon plate and embedded in the PDMS substrate. From the cross-section SEM images presented in Fig. 2, it can be seen that the AgNWs pierce the surface of the PDMS substrate and a large amount of interconnecting could be observed, resulting in the high conductivity of the AgNW/PDMS hybrid electrodes. The electrical and optical properties of the stretchable and transparent AgNW/PDMS hybrid electrodes are summarized in Fig. 4. Due to the nano-scale diameter of AgNWs, most of visible light could pass through the gap of networks, and hence the AgNW/PDMS hybrid electrodes exhibited high transparency. Certainly, the greater the AgNW content in the PDMS substrate, the greater the probability that incident light will be blocked, which is a dilemma relationship between the optical transparency and conductivity of AgNW/PDMS hybrid electrodes. Thus, the optimization of the AgNW amount is important to produce hybrid electrodes with an excellent balance between transparency and conductivity. In this work, the resistance of the stretchable AgNW/PDMS hybrid electrode could be reduced to 20 Ω sq^{-1} with transparency up to 75% (air served as the background) at 550 nm.

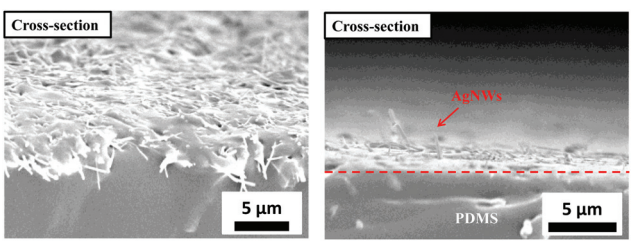

Fig. 2 SEM morphology of the AgNW/PDMS hybrid electrode.

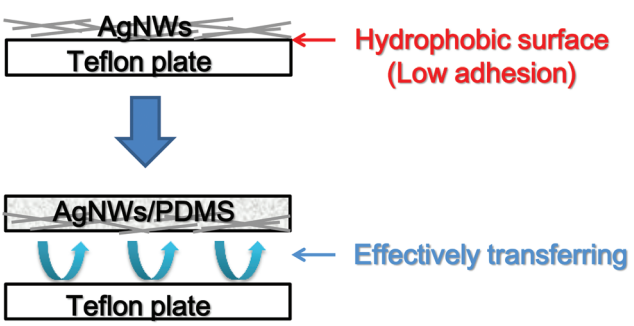

Fig. 3 Schematic representation of the transfer process.

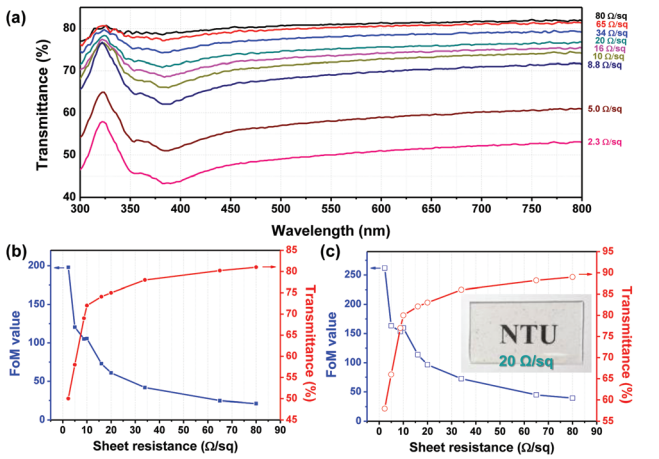

Fig. 4 The electrical and optical properties of the prepared AgNW/PDMS hybrid electrodes. (a) UV-Vis transmittance spectra of the obtained electrodes with various sheet resistances (the transmittance based on air as a reference), and FoM value plotted with sheet resistance and transmittance (T 550 nm) (b) (the transmittance based on air as a reference), and (c) (the transmittance based on the PDMS as a reference) of the stretchable electrodes.

The figure of merit (FoM) is a representative quantity used to evaluate the performance of transparent conductors,[6,33] and the FoM for transparent electrodes could be expressed by:

$$\frac{\sigma_{dc}}{\sigma_{op}(\lambda)} = \frac{Z_0}{2R_s}\frac{\sqrt{T}}{1-\sqrt{T}}$$

where σ_{dc} is the dc conductivity of the film, $\sigma_{op}(\lambda)$ is the optical conductivity at wavelength of λ nm, Z_0 is the impedance of free space (377 Ω), R_s is the sheet resistance, and T is the transmittance at λ nm. For industrial application, the FoM value should be larger than 35.[34] In this work, the FoM value of the AgNW/PDMS hybrid electrodes could reach 260 with transmittance (58%) and low sheet resistance (2 Ω sq^{-1}). Although the AgNW/PDMS hybrid film exhibited the highest FoM value of 260 at the sheet resistance of 2 Ω sq^{-1}, while we prefer to choose AgNW/PDMS hybrid electrodes with a transmittance of 83% and sheet resistance of 20 Ω sq^{-1} to conduct the following experiments for emphasizing the transparency of this kind of stretchable electrode.

Stretching, twisting, and bending behavior of the transparent AgNW/PDMS hybrid electrodes

In order to emphasize the properties and advantages between AgNWs and PDMS substrates in different harsh working environments, the stretching, twisting, and bending of the AgNW/PDMS hybrid electrodes were investigated. Fig. 5 summarizes the resistance R measured under different testing conditions by using the Digital Multimeter, R_0 = 100 Ω is the initial resistance before testing upon testing. At the stretching test, the resistance of the electrode increased during the stretching process. This result is due to the increase in length that could result in the reduction of the number of AgNWs per unit area and network density of AgNWs, which increased the resistance. This phenomenon mentioned above could be observed more clearly by using an optical microscope (as shown in Fig. S5†), while the network structure of AgNWs at 25% strain still could be retained, so that the electrode could maintain the electrical conductivity. In this work, these AgNW/PDMS hybrid electrodes could still retain conductivity even with a strain of 100% for the stretching situation.

The twisting test result demonstrated in Fig. 5b reveals that the resistance first increased slowly before reaching a twist angle of 135°. Beyond the 135° twisting, the resistance change became more significant with R up to 210 Ω at 315° twisting. However, the performance of these AgNW/PDMS hybrid electrodes at this 315° twisting was still quite prominent. This feature was enough for them to cope with the motion conditions. For the bending test, Fig. 5c shows the resistance variation of the AgNW/PDMS hybrid electrodes with different bending radii. We could see that the resistance changes very slightly during the bending tests even at the bending radius of 4.8 mm. In the process of the bending test, the influence is only at the bending part, while twisting is the comprehensive influence that makes the silver wire network difficult to maintain and silver wire contact points decrease, resulting in the obvious increase of electrode resistance.

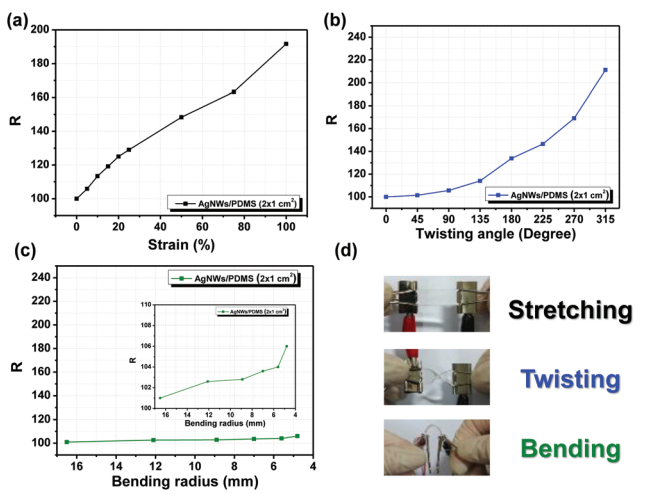

Fig. 5 The resistance variation of the AgNW/PDMS hybrid electrode for different tests: (a) stretching test, (b) twisting test, (c) bending test and (d) show the different kind of test condition.

Furthermore, the transparent and stretchable AgNW/PDMS hybrid electrode with 2 cm length was used as a segment of an external circuit preliminarily demonstrated in LED devices (as shown in Fig. 6). According to visual observations, the brightness of the LED partially weakened during 90° twisting and 20% strain, respectively, while the LED still exhibited significant brightness, clearly demonstrating that AgNW/PDMS hybrid electrodes are suitable for applications in various flexible and stretchable devices. The long-term stability in terms of R value at different testing/releasing states for these AgNW/PDMS hybrid electrodes is depicted in Fig. 7.

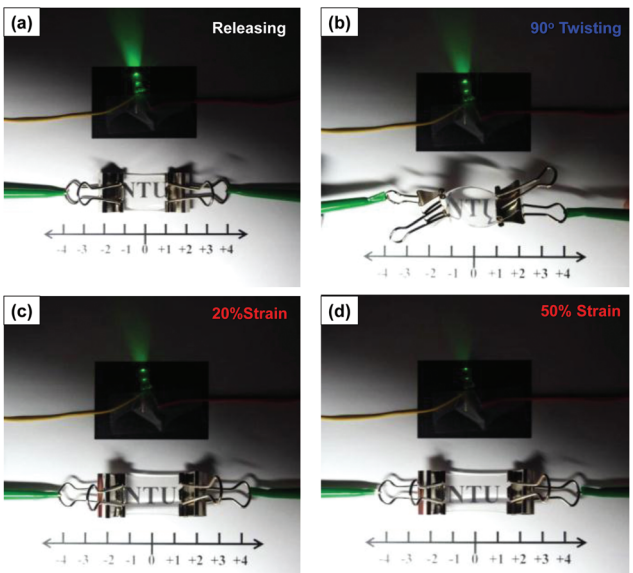

Fig. 6 LED applications of AgNW/PDMS hybrid electrodes. Photographic images of working LEDs with (a) releasing, (b) twisting, (c) strain of 50%, and (d) strain of 50% of AgNW/PDMS hybrid electrodes.

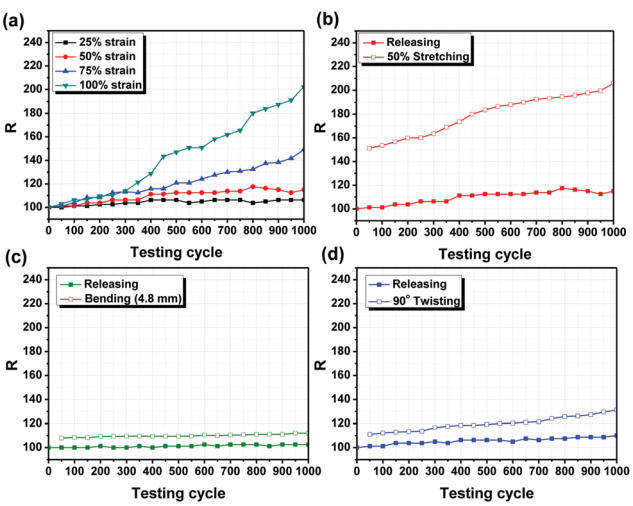

Fig. 7 The resistance variation of the AgNW/PDMS electrode for different tests: (a) releasing states of different percentages of the stretching test, (b) stretching test, (c) twisting test, and (d) bending test for 1000 cycles.

Fig. 7a exhibits the stability at different degrees of strain. The AgNW/PDMS hybrid electrode still could retain a relatively low resistance change at the strain of 50% over 1000 cycles. However, the resistance exhibited a larger rise at 100% strain over 1000 cycles. The cyclic stretching/releasing tests with the strain of 50% shown in Fig. 7b reveal that the increasing of the resistance variation at the stretching state was larger than that in the releasing state.

However, in the twisting and bending tests, this phenomenon was not so obvious (as shown in Fig. 7c and d). The sheet resistance of the AgNW/PDMS hybrid electrode could be maintained after testing (stretching, twisting and bending) for 1000 cycles.

Properties of the elastomeric electrochromic device

We used the stretchable AgNW/PDMS hybrid electrodes to prepare the elastomeric electrochromic device, and the structure of the device is shown in Fig. 8. Until now, only a small number of researchers have tried to make combinations of AgNWs and electrochromic materials.[16,35]

However, no group could successfully prepare the electrochromic device with a full AgNW electrode system because the AgNWs at the anode will be oxidized during the charge exchanging process with the electrolyte. The electrochemical properties of the AgNWs were investigated by cyclic voltammetry (CV) conducted by using the cast AgNWs on a glass slide or PDMS (12 mm × 5 mm) as the working electrode in anhydrous CH_3CN, using 0.1 M of TBAP as a supporting electrolyte under a nitrogen atmosphere. The typical CV diagrams for AgNW–glass and AgNW–PDMS are depicted in Fig. 9a for comparison. These two kinds of electrodes exhibited one irreversible oxidation peak, indicating that electrons could not be successively returned after being removed from the AgNWs.

Oxidized AgNWs would lose conductivity at the second time measurement, and the CV diagrams would not have any redox peaks. The micro characteristic of the AgNW electrode observed from the SEM images after one cyclic measurement shown in Fig. 9b demonstrates that the AgNWs could not form

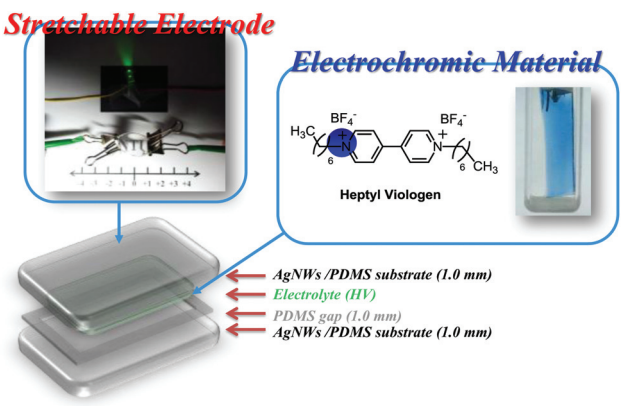

Fig. 8 Schematic diagram of the HV ECD based on the AgNW/PDMS hybrid electrodes.

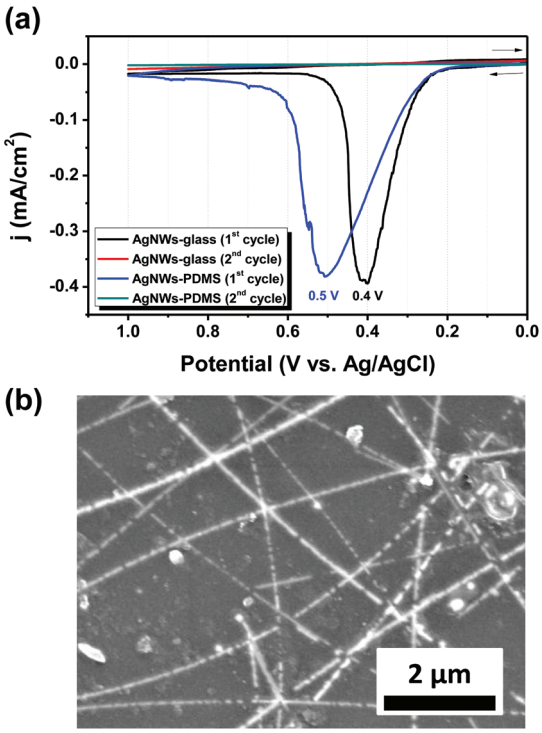

Fig. 9 (a) Cyclic voltammetric diagrams of AgNWs on the different substrates (working electrode area: 12 mm × 5 mm, sheet resistance: 20 Ω sq^{-1}) in 0.1 M TBAP/CH_3CN at a scan rate of 50 mV s^{-1}. (b) SEM of the AgNW–glass electrode scanned over 0.4 V.

a uniform network structure anymore due to breakage, and result in the loss of conductivity. For this reason, AgNWs were difficult to use as the anode electrode for the electrochromic device unless the applied potential was lower than the oxidation potential of the AgNWs. Thus, in order to overcome this problem, heptyl viologen (HV) was chosen as the electrochromic material in this study, which has relatively low redox potential and excellent electrochromic properties.

The electrochemical behavior of the HV ECD was investigated by CV and the diagrams are shown in Fig. S6.† A reversible redox step at −0.65 V could be observed from the CV diagram, meaning that the electrons could be successively passed in the circuit and transferred from the AgNW electrode to the redox center of HV. Moreover, the redox behavior could still remain even after 50 cycles. The electrochromic behavior of the HV ECD based on the AgNW/PDMS hybrid electrode was investigated and evaluated by using the combination of CV and UV-Vis instruments (spectroelectrochemical). The optical absorbance curves of the HV ECD correlated to applied potentials are depicted in Fig. 10. The device was transparent and colorless in the neutral state (0 V). Upon reduction at an applied potential of −0.65 V, the new peak at 398 nm and a broad band with a peak around 603 nm in the visible region gradually increased in intensity with the color change from transparent and colorless to blue.

The switching data for the HV ECD are demonstrated in Fig. 11. The switching time was calculated at 90% of the full

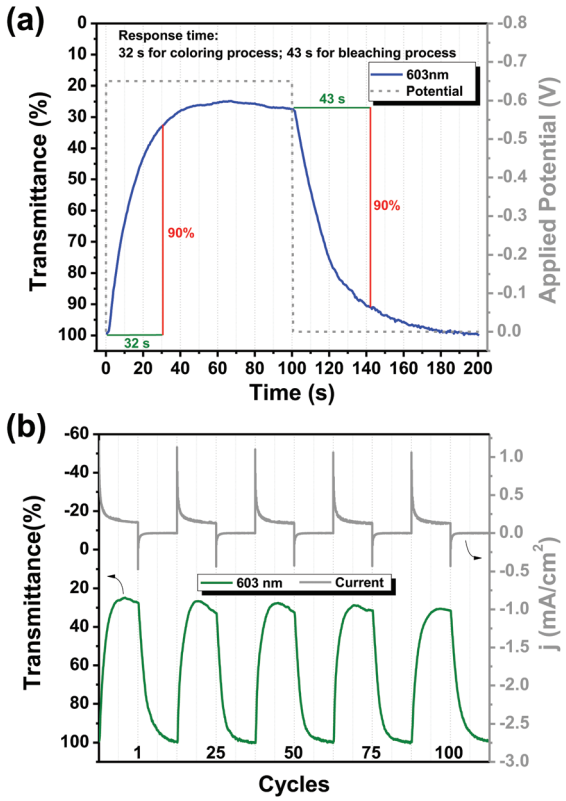

Fig. 10 (a) UV-vis spectra of the HV ECD based on the AgNW/PDMS hybrid electrode (electrochromic material: 1 mg, working area: 20 mm × 20 mm, gap thickness: 1 mm) in 0.1 M TBAP/CH_3CN at applied related potentials, and (b) photos of ECDs in the bleached state and colored state.

switch. The response time was 32 s for the coloring process, and 43 s for the bleaching process at 603 nm (as shown in Fig. 11a). The slower response time for the coloring and bleaching processes at 603 nm could be ascribed to two reasons. Firstly, the gap of the electrochromic device used in this study is 1 mm that is much thicker than the general electrochromic device with the gap around only 60 μm, resulting

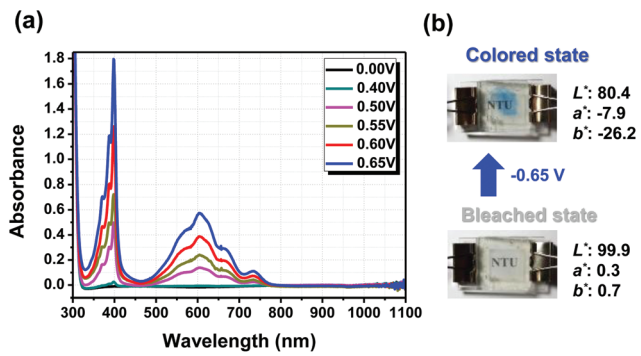

Fig. 11 (a) Calculation of the optical switching time at 603 nm at the applied potential, and (b) electrochromic switching between 0.00 V and 0.65 V with a cycle time of 100 s of the HV ECD based on the AgNW/PDMS hybrid electrode (electrochromic material: 1 mg, working area: 20 mm × 20 mm, gap thickness: 1 mm) in 0.1 M TBAP/CH_3CN.

Table 1 Optical and electrochemical data collected for coloration efficiency measurements of the HV ECD based on the AgNW/PDMS hybrid electrode

Cycling times[a]	ΔT[b]	ΔOD[c]	Q[d] (mC cm^{-2})	η[e] (cm^2 C^{-1})	Decay[f] (%)	Decay[g] (%)
1	74.5	0.60	18.89	31.82	0	0
25	73.2	0.58	18.57	31.23	1.85	3.4
50	72.3	0.56	18.03	31.06	2.39	6.7
75	70.4	0.54	17.74	30.55	3.99	10.0
100	69.3	0.51	17.55	29.29	7.95	15.0

[a] Switching between 0 and −0.65 V. [b] Transmittance change at 603 nm. [c] Optical density (ΔOD) = $\log[T_{bleached}/T_{colored}]$, where $T_{colored}$ and $T_{bleached}$ are the maximum transmittance in the oxidized and neutral states, respectively. [d] Ejected charge, determined from the *in situ* experiments. [e] Coloration efficiency is derived from the equation $\eta = \Delta A/Q$. [f] Decay of the coloration efficiency after cyclic scans. [g] Decay of the optical density after cyclic scans.

in a longer response time. Secondly, there is only a cathodic HV electrochromic material in the device without addition of any complementary anodic electrochromic material as the charge storage layer for the formation of an ambipolar system. Therefore, the response time for coloring and bleaching is longer.[36] For the durability test as shown in Fig. 11b and Table 1, the HV ECD revealed only 7.95% decay of its redox activity after 100 cycles. All of these results are sufficient to show the feasibility that AgNW/PDMS hybrid electrodes could be used as both anodic and cathodic electrodes in the ECD. To the best of our knowledge, this is the first prototype electrochromic device successfully introducing the full AgNW electrode system.

Conclusions

We demonstrated an effective and facile method to transfer AgNWs into PDMS for successfully preparing stretchable AgNW/PDMS electrodes. The obtained highly conductive AgNW/PDMS hybrid electrodes were colorless and transparent with low sheet resistance, and the conductivity could be retained even after stretching, twisting, and bending for 1000 cycles. Furthermore, a novel elastomeric HV ECD could be readily fabricated based on the stretchable AgNW/PDMS electrodes, and the prepared ECD could exhibit excellent electrochromic behavior with the color change between colorless and blue. Even after 100 switching cycles, the HV ECD could still have excellent efficacy. Thus, this innovative approach for preparing AgNW–PDMS electrodes with high transparency and stretchability should be highly competitive, and the elastomeric ECD is just a representative example to substantiate the feasibility of applications, such as wearable devices and transparent displays with foldable screens in the next generation to replace the rigid substrates.

Acknowledgements

The authors are grateful to the Ministry of Science and Technology of Taiwan for financial support.

Notes and references

1 K. Alzoubi, M. M. Hamasha, S. Lu and B. Sammakia, *J. Disp. Technol.*, 2011, **7**, 593–600.
2 S. Iijima, *Nature*, 1991, **354**, 56–58.
3 K. S. Novoselov, A. K. Geim, S. V. Morozov, D. Jiang, Y. Zhang, S. V. Dubonos, I. V. Grigorieva and A. A. Firsov, *Science*, 2004, **306**, 666–669.
4 J. Y. Lee, S. T. Connor, Y. Cui and P. Peumans, *Nano Lett.*, 2008, **8**, 689–692.
5 Nanomarket, Market Opportunities for Silver Nanowire Transparent Conductors, 2015–2022, http://ntechresearch.com/market_reports/market-opportunities-for-silver-nanowire-transparent-conductors-2015-2022.
6 S. De, T. M. Higgins, P. E. Lyons, E. M. Doherty, P. N. Nirmalraj, W. J. Blau, J. J. Boland and J. N. Coleman, *ACS Nano*, 2009, **3**, 1767–1774.
7 D. Lee, H. Lee, Y. Ahn, Y. Jeong, D. Y. Lee and Y. Lee, *Nanoscale*, 2013, **5**, 7750–7755.
8 K. Naito, N. Yoshinaga, E. Tsutsumi and Y. Akasaka, *Synth. Met.*, 2013, **175**, 42–46.
9 T. Kim, A. Canlier, G. H. Kim, J. Choi, M. Park and S. M. Han, *ACS Appl. Mater. Interfaces*, 2013, **5**, 788–794.
10 M. Ivan, N. Nuria, A. Manuel, I. Silvia and S. Jesus, *Nanotechnology*, 2013, **24**, 275603.
11 L. Li, Z. Yu, W. Hu, C. H. Chang, Q. Chen and Q. Pei, *Adv. Mater.*, 2011, **23**, 5563–5567.
12 Z. Yu, Q. Zhang, L. Li, Q. Chen, X. Niu, J. Liu and Q. Pei, *Adv. Mater.*, 2011, **23**, 664–668.
13 W. Hu, X. Niu, L. Li, S. Yun, Z. Yu and Q. Pei, *Nanotechnology*, 2012, **23**, 344002.
14 T. H. L. Nguyen, L. Quiroga Cortes, A. Lonjon, E. Dantras and C. Lacabanne, *J. Non-Cryst. Solids*, 2014, **385**, 34–39.
15 K. H. Choi, J. Kim, Y. J. Noh, S. I. Na and H. K. Kim, *Sol. Energy Mater. Sol. Cells*, 2013, **110**, 147–153.
16 H. Y. Lu, C. Y. Chou, J. H. Wu, J. J. Lin and G. S. Liou, *J. Mater. Chem. C*, 2015, **3**, 3629–3635.
17 C. Y. Chou, H. S. Liu and G. S. Liou, *RSC Adv.*, 2016, **6**, 61386–61392.
18 Y. Kim, J. Zhu, B. Yeom, M. Di Prima, X. Su, J. G. Kim, S. J. Yoo, C. Uher and N. A. Kotov, *Nature*, 2013, **500**, 59–63.
19 S. Shang, W. Zeng and X. M. Tao, *J. Mater. Chem.*, 2011, **21**, 7274–7280.
20 M. Park, J. Im, M. Shin, Y. Min, J. Park, H. Cho, S. Park, M.-B. Shim, S. Jeon, D.-Y. Chung, J. Bae, J. Park, U. Jeong and K. Kim, *Nat. Nanotechnol.*, 2012, **7**, 803–809.
21 K. Y. Chun, S. H. Kim, M. K. Shin, Y. T. Kim, G. M. Spinks, A. E. Aliev, R. H. Baughman and S. J. Kim, *Nanotechnology*, 2013, **24**, 165401.
22 K. H. Kim, M. Vural and M. F. Islam, *Adv. Mater.*, 2011, **23**, 2865–2869.
23 M. Chen, T. Tao, L. Zhang, W. Gao and C. Li, *Chem. Commun.*, 2013, **49**, 1612–1614.
24 S. Yun, X. Niu, Z. Yu, W. Hu, P. Brochu and Q. Pei, *Adv. Mater.*, 2012, **24**, 1321–1327.
25 J. Wang, C. Yan, W. Kang and P. S. Lee, *Nanoscale*, 2014, **6**, 10734–10739.
26 T. Cheng, Y. Z. Zhang, W. Y. Lai, Y. Chen, W. J. Zeng and W. Huang, *J. Mater. Chem. C*, 2014, **2**, 10369–10376.
27 M. S. Miller, J. C. O'Kane, A. Niec, R. S. Carmichael and T. B. Carmichael, *ACS Appl. Mater. Interfaces*, 2013, **5**, 10165–10172.
28 J. H. Wu and G. S. Liou, *Adv. Funct. Mater.*, 2014, **24**, 6422–6429.
29 K. E. Korte, S. E. Skrabalak and Y. Xia, *J. Mater. Chem.*, 2008, **18**, 437–441.
30 D. H. Kim, R. Ghaffari, N. Lu and J. A. Rogers, *Annu. Rev. Biomed. Eng.*, 2012, **14**, 113–128.
31 D. H. Kim, N. Lu, Y. Huang and J. A. Rogers, *MRS Bull.*, 2012, **37**, 226–235.
32 J. J. Richardson, D. Estrada, S. P. DenBaars, C. J. Hawker and L. M. Campos, *J. Mater. Chem.*, 2011, **21**, 14417–14419.
33 G. Haacke, *J. Appl. Phys.*, 1976, **47**, 4086–4089.
34 S. Sophie, E. L. Philip, D. Sukanta, C. D. Janet and N. C. Jonathan, *Nanotechnology*, 2012, **23**, 185201.
35 C. Yan, W. Kang, J. Wang, M. Cui, X. Wang, C. Y. Foo, K. J. Chee and P. S. Lee, *ACS Nano*, 2014, **8**, 316–322.
36 J. H. Wu and G. S. Liou, *Adv. Funct. Mater.*, 2014, **24**, 6422–6429.